UC San Diego

UC San Diego Electronic Theses and Dissertations

Title

NF kappa B expression and matrix metalloproteinase activity in hypertension

Permalink

https://escholarship.org/uc/item/38x7h314

Author

Wu, Kwan-I

Publication Date

2009

Peer reviewed|Thesis/dissertation

eScholarship.org Powered by the California Digital Library
University of California

UNIVERSITY OF CALIFORNIA, SAN DIEGO

NF kappa B Expression and Matrix Metalloproteinase Activity in Hypertension

A thesis submitted in partial satisfaction of the
requirements for the degree Master of Science

in

Bioengineering

by

Kwan-I Wu

Committee in charge:

Professor Geert W. Schmid-Schönbein, Chair
Professor Daniel T. O'Connor
Professor Marcos Intaglietta

2009

Copyright

Kwan-I Wu, 2009

All rights reserved

The Thesis of Kwan-I Wu is approved, and it is acceptable in quality and form for publication on microfilm and electronically:

_____

_____

_____

Chair

University of California, San Diego

2009

Table of Contents

List of Figures

Acknowledgement

First, I would like to acknowledge my advisor, Dr. Geert Schmid- Schönbein, for helping me within these two years. He taught me not only the skills of research studies and thesis writing, but also the way to think about the questions as an engineer. Without his guidance, there is no way I would have completed this thesis at all.

I would also like to acknowledge Dr. Edward Tran, who guided me through all the experimental processes. I want to thank him for his patience and constantly providing feedback to me on my works.

I would also like to thank all my dear lab partners, Marisol Chang, Amy Chan, Shakti Valdez, Nongluk Plongthongkum, Angelina Altshuler, and Jason Chow for their friendship, support, and help throughout the entire process.

Last, but not least, I would like to thank my dad, mom, and my brother for their support all the time. I would also like to thank all my Taiwanese friends here in San Diego, Christine, Winnie, shoes, Morris, Solti, and especially Howard, for being there for me, in good times and in bad times. Moreover, special thanks to Elisa, Jamie, Yelena, Penny and Ching-Tzu for being my safety net for so many years. Without them, I would not have been able to complete my studies in UCSD and this thesis.

ABSTRACT OF THE THESIS

NF kappa B Expression and Matrix Metalloproteinase Activity in Hypertension

by

Kwan-I Wu

Master of Science in Bioengineering

University of California, San Diego, 2009

Professor Geert W. Schmid- Schönbein, Chair

Hypertension is a major risk factor for cardiovascular disease, kidney failure and stroke. Recently, increasing evidences suggest a strong association between inflammation and hypertension. On the other hand, NF-κB is a common transcription factor involved in inflammatory response and overexpressed in different end-organ damage.

The objective of this study is to examine the role of NF-κB in hypertension. NF-κB expression level and translocation were compared between Wistar Kyoto rat (WKY) and spontaneously hypertensive rat (SHR) kidney, heart and brain. In addition, the animals were treated with a NF-κB inhibitor, pyrrolidine

dithiocarbamate (PDTC), for ten weeks. To determine the correlation between NF-κB and MMP, MMP-2 and -9 activities were examined after treatment.

Immunohistochemistry results showed that NF-κB expression level is significantly increased in SHR in renal glomerular and tubulointerstitial areas and brain hypothalamus compared to that in WKY ($p < 0.05$), but not in myocardium and cerebral cortex. Significant NF-κB translocation into the nucleus was found in renal tubular cells, cardiac muscle cells, and arterioles of kidney and brain in SHR.

After PDTC treatment, the systolic blood pressure was suppressed in SHR by 36 %. NF-κB expression level in treated-SHR was also decreased in renal glomerular and tubulointerstitial areas and hypothalamus compared to non-treated animals ($p < 0.05$). Also, MMP-2 and -9 activities were reduced by PDTC in SHR after treatment. The higher MMP-9 activity in SHR was also significantly decreased by PDTC ($p < 0.01$). These results suggest NF-κB is an important factor in hypertension and may be responsible for MMP activity.

Chapter 1: Introduction

Hypertension is defined by the National Institute of Health as a chronic condition with arterial blood pressure about 140/ 90 mmHg (12). It has been recognized as a multi-factorial disease resulting from the effect of a combination of genetic and environmental factors (6,28). Chronic hypertension is associated with enhanced risk for serious cardiovascular disease, including atherosclerosis, stroke, and renal failure.

Among many model of hypertension available today (13,21,31), my thesis will be focused on a genetic form of hypertension, the spontaneously hypertensive rat and its normotensive control, the Wistar Kyoto rat (36). This model of hypertension develops without any further intervention in our living environment a chronically elevated arterial blood pressure.

1.1 The Link between Chronic Hypertension and Inflammation

Recently, increasing evidence has been advanced to suggest a strong association between inflammation and hypertension. For example, a strong indicator for chronic inflammation is derived from the evidence for elevated levels of activated neutrophils, monocytes, and other leukocytes in the circulation, including the expression of iNOS, and other vascular inflammatory markers in spontaneously hypertensive rats (SHR) than in Wistar-Kyoto rats(WKY)(4,23,44). Rodriguez-Iturbe et al. (2005) also found lymphocyte and macrophage infiltration and oxidative stress specifically in tubulointerstitial areas of the kidney, which might play

an important role in the development and maintenance of hypertension in SHR (40). Leukocytes from hypertensives have an enhanced cytotoxicity and they exhibit spontaneous degranulation of their neutrophils (47) Another marker for enhanced inflammation is the presence of oxygen free radical production (14,30) as well as extensive apoptosis(26) .

This suppression of acute inflammation may lower the blood pressure in some situation. For example, Bataillard et al.(1995) treated Lyon hypertensive rats with silica, which is a selective toxin to macrophages *in vivo*. The silica-treated rats showed lower blood pressure and decreased left ventricle weight, indicating the attenuation effect on hypertension by silica treatment(3).

1.2 The Link between Chronic Hypertension and End-Organ Damage

Epidemiological evidence indicates that hypertensive patients are at major risk for cardiovascular disease, kidney failure and stroke (28). This is one of the major reasons why there is the need for an understanding of the molecular mechanism that lead to arterial hypertension. Besides the high blood pressure, hypertension exhibit cardiovascular lesions and many pathophysiological process, such as endothelial activation, inflammation, thrombogenesis, activated renin-angiotensin-aldosterone system, may also contribute to the development of end-organ damage.(12) For example, Luft et al (1999) first used dTGR rat model, which is crossed transgenic of the human angiotensionogen and renin genes, to demonstrate such effect. These investigators found that the rats developed moderately sever hypertension and died of end-organ cardiac and renal damage by

week 7. Sections of the kidney and heart also showed fibrinoid thrombi in vessels and patchy areas of necrosis (31).

1.3 The Link between Hypertension and Matrix Metalloproteinase (MMP)

There are many studies pointing to an association between MMPs, particularly MMP-2 and MMP-9, and hypertension, based on the fact that MMPs proteolytic system and TIMPs are involved in the regulation of extracellular matrix (ECM) structuring. However, the role of MMPs in hypertension is not been fully understood. Some studies showed elevated mRNA for MMP-2 and MMP-9, and increased MMP-2 protein level especially in juxtamedullary cortex, which may be responsible for renal interstitial fibrosis in SHR (7,20). Other studies showed depression of active MMP-2 and MMP-9 in plasma of hypertensive patients, which suggested that decreased MMP-2 and -9 activities may induce excessive accumulation of ECM components resulting in fibrosis on the vascular wall (42). Recent evidence, however, suggests that activation of MMP-2 and -9 in the microcirculation affects not only blood pressure in hypertension but also accounts for diverse cell dysfunction by a receptor cleavage mechanism (12).

1.4 Matrix Metalloproteinase

The MMPs are a family of 24 structurally related enzymes found in vertebrates. MMPs are zinc-containing enzymes that can degrade the extracellular

matrix (ECM) and connective tissue proteins (17,52). Based on their substrate specificity, primary structure and cellular location, the MMPs have been classified into collagenases, gelatinases, stromelysins, membrane-type, and matrilysins (11). In general, MMPs consist of a signal peptide, a propeptide, a catalytic domain, a hinge region and, in the majority of cases, a C-terminal domain. The propeptide contains an invariant Cys residue, which chelates the active zinc site to maintain proMMP zymogen form. The propeptides need to be cleaved from the enzyme for MMPs activation. The catalytic domain contains a HEXGHXXGXXH zinc-binding sequence, providing the binding site for its specific substrate (11,39). The hinge regions link catalytic domain to C-terminal domain, which is involved in mediating protein-protein interactions (52). Many studies have shown that MMPs play an important role in different physiological or pathological function, including vascular modeling, cellular migration and regulating ECM proteins and adhesion molecules due to its proteolytic ability (17,39,52).

Under normal physiological conditions, the activities of MMPs are precisely regulated by gene transcription and synthesis of precursor zymogens, interactions with specific ECM components, and inhibition by metalloproteinase inhibitors (TIMPs) (49). Loss of activity control or the imbalance between MMPs and TIMPs may result in numerous physiological diseases, such as cardiovascular diseases, inflammation and cancer (39).

1.4.1 MMP-2 and MMP-9

MMP-2 (gelatinase-A) and MMP-9 (gelatinase-B) are both in the gelatinase

subgroup of MMPs and mainly digest denatured collagens (gelatins). They have three repeats of type II fibronectin domain inserted in the catalytic domain, which can bind to gelatin, collagens, and laminin (1). The induction of MMP-2 and MMP-9 can be influenced by a variety of chemical agents and cytokines, such as IL-1 (16,27) and possibly through the formation of transcription factors that bind to specific response elements on MMP gene promoters. Activator protein -1(AP-1) is one of the common response element contained within the promoter region of certain MMP genes, which provided the evidence of gene regulation in MMPs expression by transcription factors. In addition, there was another study that demonstrates the overexpression of IκBα can almost completely inhibited expression of MMP-9, since nuclear factor-κB site has been identified on the MMP-9 promoter region (5).

1.5 Nuclear Factor Kappa B

Nuclear factor-kappaB (NF-κB) proteins were first discovered in the lab led by Dr. Baltimore in 1986 and identified as a B-cell nuclear factor based on its ability to bind to an 11-base pair sequence in the immunoglobulin κ-light-chain enhancer in B cells(46). The NF-κB proteins comprise a family of dimeric transcription factor (e.g., c-Rel, RelA (p65), RelB, C-Rel, and Dorsal, Dif in *Drospophila*) sharing an approximately 300 amino-acid Rel regions (Rel homology domain, RHD) including DNA-binding and dimerization domains, nuclear translocation signal (NLS), and the binding site of IκB inhibitors(51). IκB inhibitors (e.g., IκBα,–β, –ε, –γ, p105 and p100) are also in the NF-κB family due to their ability to bind to NF-κB dimers in the

inactivation stage. It has be found that these proteins have long C-terminal domains containing multiple copies of ankyrin repeat, which can be removed by proteasome-mediated proteolysis (18).

1.5.1 Mechanism of Activation

In resting cells, NF-κB presents as IκB-bound complex in the cytoplasm. Upon activation by extracellular stimuli, IκBα is phosphorylated by IκB kinase (IKK) and further proteolytically degraded by proteasomes and other proteases. This process can allow NF-κB to translocate from cytoplasm into the nucleus. In the nucleus, activated NF-κB dimers can bind to 9-10 base pair DNA sites (5'-GGGRNWYYCC-3'; R, A or G; N, any nucleotide; W, A or T; Y, C orT), also called κB sites, and regulate specific gene expression (10). On the basis of great variety of κB sites, protein-protein interaction with other promoters, and physiological conditions, the NF-κB family proteins can form either homodimers or heterodimers in vivo, except for RelB, which only forms heterodimers. p50-p65 heterodimer is the major NF-κB dimer in many cells (18,19).

1.5.2 NF-κB and Inflammation

Inflammation is present when cells are exposed to life-threatening conditions, such as UV light, oxygen radicals, viruses, cytokines, and serves a tissue repair mechanism. In this case, many genes can be newly activated and generate products to defend the organism (45). The inflammatory process consists of a sequence of

events including increased permeability and blood flow, immune cells infiltration, cell necrosis and apoptosis, generation of new humoral mediators for cell growth, etc. (43). Many studies have provided evidence that NF-κB is responsible for regulating numerous genes of the inflammatory cascade (34,45). By studying at the molecular level, Chen et al. (1995) have shown the promoters of the E-selectin, vascular cell adhesion molecule-1 (VCAM-1), and intercellular adhesion molecule-1 (ICAM-1) genes, which are associated with leukocytes rolling and adhesion, contain recognition sequences for the inducible NF-κB. Also, the cell-surface expression of E-selectin, VCAM-1, and ICAM-1 has been up-regulated coming with cytokine and LPS induction by inhibiting IκB proteolysis (9).

1.5.3 NF-κB in End-Organ Damage

Since the failure of inflammatory cascade to reach resolution may potentially lead to organ dysfunction and cell death, and the fact that a much larger variety of diseases are highly related to inflammation, it is not surprising to see that NF-κB plays a leading role in some end-organ damage (20,43). Several studies have shown that NF-κB activation is one of the prominent features in either damaged kidneys or disordered hearts. The evidence includes upregulation of p65 mRNA, increased NF-κB binding activity, and elevated IKK activity. (20,31,33)

1.5.4 Inhibition of NF-κB Activation

There are numerous inhibitor of NF-κB with multiple reaction mechanisms,

such as stabilizing IκB or directly blocking IκBdegradation, inhibiting IKK complex from activation, and downregulation of NF-κB functions including nuclear translocation and DNA binding ability (19). Through cell culture experiments, certain metal chelators and dithiocarbamates are shown to inhibit NF-κB activation. In particular, a pyrrolidine derivative of dithiocarbamate (PDTC) was investigated in detail and found as a potent inhibitor on the transactivation of various reporter genes regulated by NF-κB (45).

However, the complete mechanism of PDTC is not well understood yet since it has several biological effects that have been considered, including the interference with reactive oxygen metabolism (25,42) and the chelation of divalent metal ions (50). These prooxidant and metal-chelating properties may be involved in its ability to inhibit NF-κB activation.(37) Several studies have shown some characteristics of the inhibiting effect of PDTC on NF-κB activation. They found that PDTC most likely stabilizes IκB to prevent the release of NF-κB rather than acting on the level of cytoplasmic NF-κB-IκB complex or interfering with DNA binding.(20,45)

Even though the mechanism of the inhibiting effect of PDTC on NF-κB ▪ requires further studies, it has shown to attenuate hypertension in different cases, such as attenuation of hypertrophy (20,29), and end-organ damage in the double transgenic rats(dTGR) (35), and to suppress inducible nitric-oxide synthase, infiltration of immune cells, and superoxide anion formation in SHR model (22,23,41).

1.6 Goals of this Investigation

The overall aim of this study is to further examine the role of NF-κB in hypertension. There are several studies showing that NF-κB is involved in inflammation.(2) In addition, evidence for an association of hypertension and inflammation as well as end-organ damage have been provided recently (4,23,44). Hence, we hypothesize that NF-κB may be involved in the inflammatory process leading to end-organ damage in hypertension. Most of the studies on NF-κB in hypertensive models were focused on the kidney (31,40); few studies exist on other organs in the SHR. In order to further investigate the involvement of NF-κB with end-organ damage in the SHR model, three major organ tissues, kidney, heart, and brain were chosen for the study base on their association with high blood pressure and other pathological factors.(28) In this study, immunohistochemistry was performed to determine the difference of NF-κB expression level in SHR compared to the Wistar-Kyoto rat (WKY). The primary antibody we chose for immunohistochemistry is an anti-NF-κB p65 subunit, because p50-p65 heterodimer is the major NF-κB dimer in many cells. Based on the recent evidence from our lab, which indicates that activation of MMP-2 and MMP-9 in the microcirculation could account for diverse cell dysfunction in hypertension (15), we hypothesized that NF-κB may be the upstream factor that controls MMPs activity leading to end-organ damage in SHR. In this study, we applied PDTC, a NF-κB inhibitor, into animals' daily water and examined MMP-2 and MMP-9 activity at the end of

the treatment. Although some studies have shown the suppressing effect of PDTC on blood pressure in SHR(20,22,40), the underlying mechanism remains unclear.

1.6.1 Objective

The objective of this thesis is to determine the role of NF-κB in hypertension and its effect on MMP expression using hypertensive rats (SHR) and normotensive rats (WKY) models.

1.6.2 Hypothesis

We hypothesize that NF-κBexpression levels are elevated in SHR kidney, heart, and brain, important organs associated with inflammation and organ dysfunction in hypertension. The NF-κB level decrease after treatment with the NF-κB inhibitor, PDTC. Furthermore, we hypothesize that MMP activity in SHR plasma can be attenuated after PDTC treatment, since the suppression of NF-κB may have an effect on either expression or activation of MMPs.

1.6.3 Specific Aims

1. **Determine the NF-κB expression levels in SHR and normotensive WKY rats**

a. Compare NF-κB expression levels in SHR and WKY by immunohistochemistry in kidney, heart and different region of brain.

b. Determine nuclear translocation of NF-κB in SHR and WKY.

2. **Determine the effect of PDTC on SHR and WKY rat blood pressure and NF-κB ▪ expression levels**

a. Determine the systolic blood pressure in PDTC-treated and non-treated animal groups.

b. Determine by immunohistochemistry NF-κB expression levels in SHR and WKY with and without PDTC treatment.

3. **Determine the effect of PDTC on MMP activity**

a. Compare MMP-2 and MMP-9 activity in SHR and WKY with and without PDTC treatment by gelatin gel zymography.

Chapter 2 Methods

2.1 Animals

The experimental protocol was reviewed and approved by the University of California, San Diego Animal Subjects Committee. Male SHR at 13-15 weeks of age and their normotensive controls, the Wistar Kyoto (WKY) (Charles River Laboratories, Wilmington, MA, USA) of comparable age were first tranquilized with Xylazine (20 mg/ml, 200 μl / kg bodyweight i.m) (MWI, Nampa, ID). After 15 minutes, general anesthesia was administered (Nembutal, 50 mg/ml, 1 ml/ kg bodyweight, i.m.) (Pentobarbital Sodium Injection, Ovation Pharmaceuticals, Inc.,Deerfield, IL). After 15 minutes, reflex level was tested with a tail pinch to assure a surgical level of anesthesia. Polyethylene(PE) catheters (PE50, I.D. 0.5mm/ O.D. 0.956 mm, Becton Dickinson Primary Care Diagonistics, Sparks, MD) were placed into the femoral artery and femoral vein prior to start of surgery. The systolic blood pressure was recorded by a laboratory computer (Power Macintosh G3 with MacLab, Apple Computer Company, Cupertino, CA). Supplemental doses of anesthesia were administered intravenously at a dose of 5 mg/kg as needed after reflex testing. Body temperature was maintained at 37°C by a water-heated animal stage. At the end of study, the animals were euthanized (sodium pentobarbital 120 mg/kg body weight, i.v.).

2.2 Treatment protocol

Subgroups of the WKYs and SHR rats were treated with NF-κB inhibitor, pyrrolidine dithiocarbarmate (PDTC, 150 mg/kg/day ; Sigma-Aldrich, St.Louis,

MO). The drug was given in drinking water for a period of 10 weeks. Untreated group received standard chow and water.

2.3 Determination of Systolic Blood Pressure

Two animals from each group were measured by the tail-cuff method. The blood pressure was measured every week by the same person and at the same time of day.

2.4 Tissue Preparation and Embedding

After the tissues were removed from the animals, they were cut and embedded in Tissue-Tek O.C.T. (Optimal Cutting Temperature) Compound (Sakura Finetek, Torrance, CA). A small portion of each tissue was placed in O.C.T. compound and quickly frozen by immersed into 2-methylbutane chilled in liquid nitrogen. The portions collected of each tissue have been shown in Figure 2-1. The frozen tissue will be stored at -20°C before sectioning.

2.5 Tissues Sectioning

Each tissue sample was sectioned using a Leica CM 3500 cryostat onto Fisherbrand Superfrost Plus Microscope Slides (Fisher Scientific, Pittsburgh, PA). Section thickness was fixed at 10 μm for brain, and 5μm for kidney and heart. Each slide has one WKY sample and one SHR sample side by side to maintain standard conditions for all further analysis. Slides were then stored at -20°C until use.

2.6 Immunohistochemical Labeling of NF-κB

Brain

Frozen sections were fixed with methanol at -20°C for 5 minutes. Endogenous peroxidase was quenched by peroxidase blocking solution (Peroxo-Block; invitrogen, Carlsbad, CA) for 45 seconds. Non-specific immune-adsorption was blocked by incubation with 5 % goat serum in PBS-T (0.1% Triton X-100 in PBS) for 1 hour. The sections were then labeled with anti- NF-κB p65 rabbit polyclonal antibody (sc-109, Santa Cruz Biotechnology, Santa Cruz, CA) (1:50 in 5% goat serum in PBS-T, v/v) for 2 hour at room temperature. This antibody recognized both the inactive form of p65 subunit, bound to p50 and IκB in the cytoplasm, and the active monomeric form in the nucleus. Controls for immunostaining included buffer alone or nonspecific purified rabbit immunoglobulin G (IgG). Sections were washed three times in PBS-T before ImmPRESS peroxidase reagent (ImmPRESS anti-rabbit Ig peroxidase kit; Vector Laboratories Inc., Burlingame, CA) was used as secondary antibody. Peroxidase activity was visualized with diaminobenzidine (DAB) substrate (Vector Laboratories Inc.). Selected tissue sections were counterstained for location of cell nucrlei (VECTASHIELD mounting medium with DAPI, Vector Laboratories Inc.)

Heart and Kidney

Frozen sections were fixed in acetone at -20°C for 10 minutes. Endogenous peroxidase was quenched by peroxidase blocking solution (Peroxo-Block;

Invitrogen, Carlsbad, CA) for 45 seconds. Non-specific adsorption was blocked by incubating the sections with 5 % goat serum in TBS (2.4gm Tris-HCl, 8.76gm NaCl to 1 Liter, pH=7.4) for 1 hour. The sections were then labeled with anti-NF-kB p65 rabbit polyclonal antibody (sc-109, Santa Cruz Biotechnology, Santa Cruz, CA) (1:50 in 5% goat serum in TBS, v/v) for 1.5 hour at room temperature. This antibody recognized both the inactive form of p65 subunit, bound to p50 and IκB in the cytoplasm, and the active monomeric form in the nucleus. Controls for immunostaining included buffer alone or nonspecific purified rabbit immunoglobulin G (IgG). Sections were washed three times by PBS-T before ImmPRESS peroxidase reagent (ImmPRESS anti-rabbit Ig peroxidase kit; Vector Laboratories Inc.) was used as secondary antibody. Peroxidase activity was visualized with DAB substrate (Vector Laboratories Inc.). Selected sections were counterstained with DAPI (VECTASHIELD mounting medium with DAPI, Vector Laboratories Inc.).

2.7 Gelatin Gel Zymography Protocol

Gelatin zymography was carried out with 0.6 µl of animal plasma, which was freshly collected and frozen (-20°C) until measurements. Gelatinolytic activity was visualized as clear bands of lysis against a dark background on gelatin containing polyacrylamide gels (Bio-Rad Laboratories, Hercules, CA). SDS gels (10% degassed Acrylamide/ Bis) with gelatin (0.8 mg/ml) were loaded with plasma samples and run (~120V, constant voltage) until bromophenol blue tracking dye reaches the bottom of the gel. The gels were incubated in the renaturing buffer

(2.5% v/v triton x-100) during gentle agitation for 60 minutes at room temperature. The gels were then incubated in the developing buffer under 37°C overnight for maximum sensitivity. In order to see clear bands of MMP-9, 2 µl of animal plasma were loaded and the gels were incubated in the developing buffer for 2 hours. The gels were stained with Coomassie Blue R-250 for 45 minutes and then de-stained (destaining buffer with Methanol : Acetic acid : Water, 50 : 10 : 40 ratio) until areas of gelatinolytic activity appear as clear sharp bands (where the protease had digested the gelatin) over the blue background.

2.8 Data Analysis

Image Analysis

The images of the sections were digitized and processed with Image J (NIH, http://rsbweb.nih.gov/ij/). In order to eliminate the background and generate new images for light absorption analysis, the following equation is used for each pixel:

$I_I' = (I_I - I_D) / (I_B - I_D) * 255$

I_I'= new image

I_I = pixel intensity on the image

I_B = pixel intensity without section

I_D = pixel intensity when no microscope light is on

Then the new images were inverted and converted into grayscale for further analysis. Since only tissue area was used for light absorption measurement, areas on the sections without tissue were set to an intensity of zero and used as a lower threshold.

In order to get average value of light intensity over the tissue and exclude

the areas without tissue, the following equations are used:

$I_{Threshold}$ = (255* ΣA tissue + 0* ΣA empty) / (ΣA tissue + ΣA empty)

$I_{gray\ tissue}$= (ΣI tissue + ΣI empty) / (ΣA tissue + ΣA empty)

ΣA tissue: total tissue area

ΣA empty: total area without tissue

ΣI tissue: total pixel intensity of tissue

ΣI empty: total pixel intensity of area without tissue

$I_{Threshold}$ and $I_{gray\ tissue}$ were measured with the program and then the total tissue pixel intensity and the total tissue area can be calculated from these two equations respectively. The immunohistochemical label intensity is derived by taking the total tissue pixel intensity divided by total tissue area.

Statistical Analysis

All measurements are presented as mean ± standard deviation. Comparisons of mean values between animal groups were carried out by two-tailed student's t-test. Two-factor ANOVA was used to compared blood pressure with the multiple animal groups and the time courses. $p < 0.05$ was considered statistically significant.

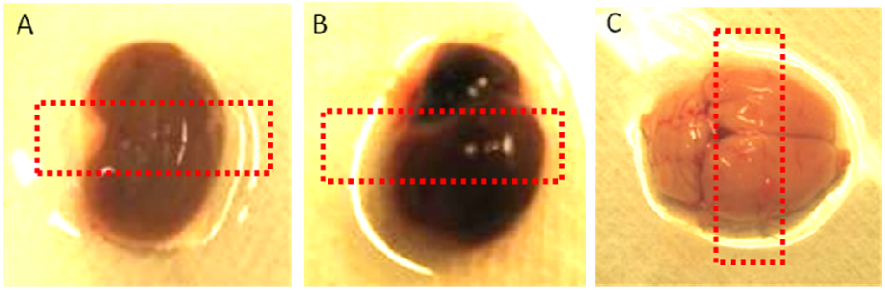

Figure 2-1. Freshly harvested rat organs: A. Kidney B. heart, C. brain. Red dash line boxes indicate approximate areas of tissue used for immunohistochemistry.

Chapter 3 Results

3.1 NF-κB expression level

NF-κB expression level was detected by immunohistochemistry with primary anitibody against NF-κB p65 subunit in kidney, heart and brain. The SHR had significantly higher expression ($p < 0.05$) in renal glomerular and tubulointerstitial areas on average by 14% (Fig. 3-1), and in hypothalamus region of brain by 22% (Fig.3-4) compared with WKY. The NF-κB expression levels were not significantly increased ($p > 0.05$) in SHR in myocardium (Fig. 3-2) and cerebral cortex (Fig. 3-3).

3.2 Translocation of NF-κB

NF-κB label density was measured in both the nucleus and the cell cytoplasm. In renal tubular cells, SHR has a significantly higher NF-κB label density in the nucleus, and there are no differences in cytoplasm between WKY and SHR (Fig.3-5A). There were no differences of NF-κB label density in cytoplasm between WKY and SHR in cells of renal blood vessel wall. But SHR has significantly elevated label density in the nucleus than in cytoplasm (Fig. 3-5B). In cardiac muscle cells, SHR showed significantly increased label density in the nucleus than in cytoplasm (Fig. 3-6A) while WKY and SHR have similar level of label density in cytoplasm. No differences were found between either WKY and SHR or nucleus and cytoplasm in blood vessels of myocardium (Fig. 3-6B). Significantly higher expression in the nucleus of SHR brain was detected in

hypothalamus region and cells of blood vessel wall but not in cerebral cortex (Fig. 3-7).

3.3 Suppression of blood pressure by PDTC treatment

Systolic blood pressure in SHRs started to significantly decreasing in the second week of PDTC treatment compared with non-treated SHR (153 ±7 and 163 ±5 mmHg, respectively). The time course of blood pressures in SHR during the treatment also showed a significant difference compared to the non-treated SHR (Fig. 3-8). The systolic blood pressure at the end of the treatment was 120 ±3 mmHg in PDTC-treated SHR and 188 ±4 mmHg in non-treated SHR, whereas the systolic blood pressure of the PDTC-treated and non-treated WKY are 115 ±4 mmHg and 114 ±2 mmHg, respectively.

3.4 NF-κB expression level after PDTC treatment

The NF-κB expression level after PDTC treatment was significantly decreased by 12 % compared with non-treated SHR in renal glomerular and tubulointerstitial areas (Fig. 3-9) and brain hypothalamus (Fig. 3-12), whereas no significant difference were detected between PDTC-treated WKY and non-treated WKY.

3.5 Attenuation of MMP activity by PDTC treatment

The MMP-2 and MMP-9 activities in plasma were examined by gelatin gel zymography. There was no difference in both pro-MMP-2 and active MMP-2

between WKY and SHR. But MMP-2 activity was suppressed in both WKY and SHR after PDTC treatment by 14% and 8%, respectively (Fig.3-13A). The pro-MMP-2 activity was only suppressed by PDTC in SHR but not in WKY (Fig. 3-13B).

The SHR has elevated MMP-9 activity compared with WKY. During PDTC treatment, the MMP-9 activity was found to be suppressed in SHR but not in WKY, and the activity was also significantly lower than treated-WKY (Fig. 3-14). As control, both MMP-2 and MMP-9 activity were blocked *in-vitro* by metal chelation (EDTA).

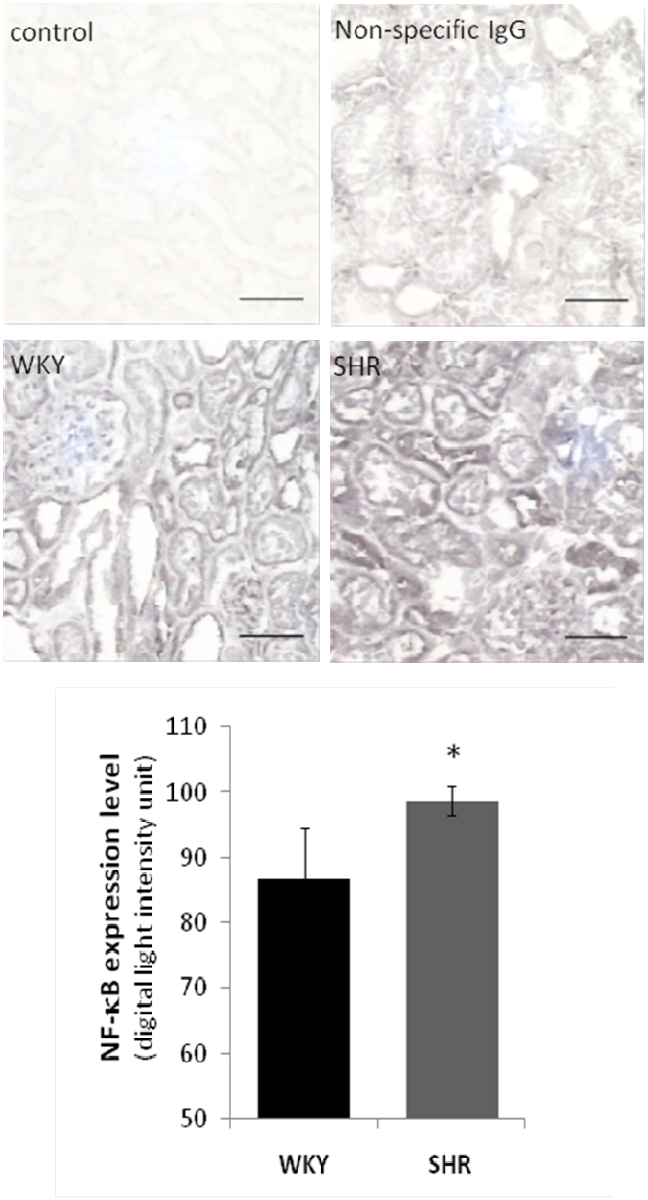

Figure 3-1. (Top panels) Micrographs of frozen immunohistochemical sections with primary antibody against NF-κB p65 subunit expression as seen by DAB substrate in renal glomerular and tubulointerstitial areas. *Control* is without primary antibody, *non-specific IgG* is with an irrelevant primary antibody and *WKY* and *SHR* is for Wister-Kyoto and Spontaneously Hypertensive Rat, respectively. Scale bar = 100 μm. (Bottom bar graph) Light absorption measurements over whole tissue expressed as digital units. The SHR has higher expression of NF-κB p65 subunit in renal cortex. N=4 rats for each group. *p <0.05 compared to WKY in student's t-test.

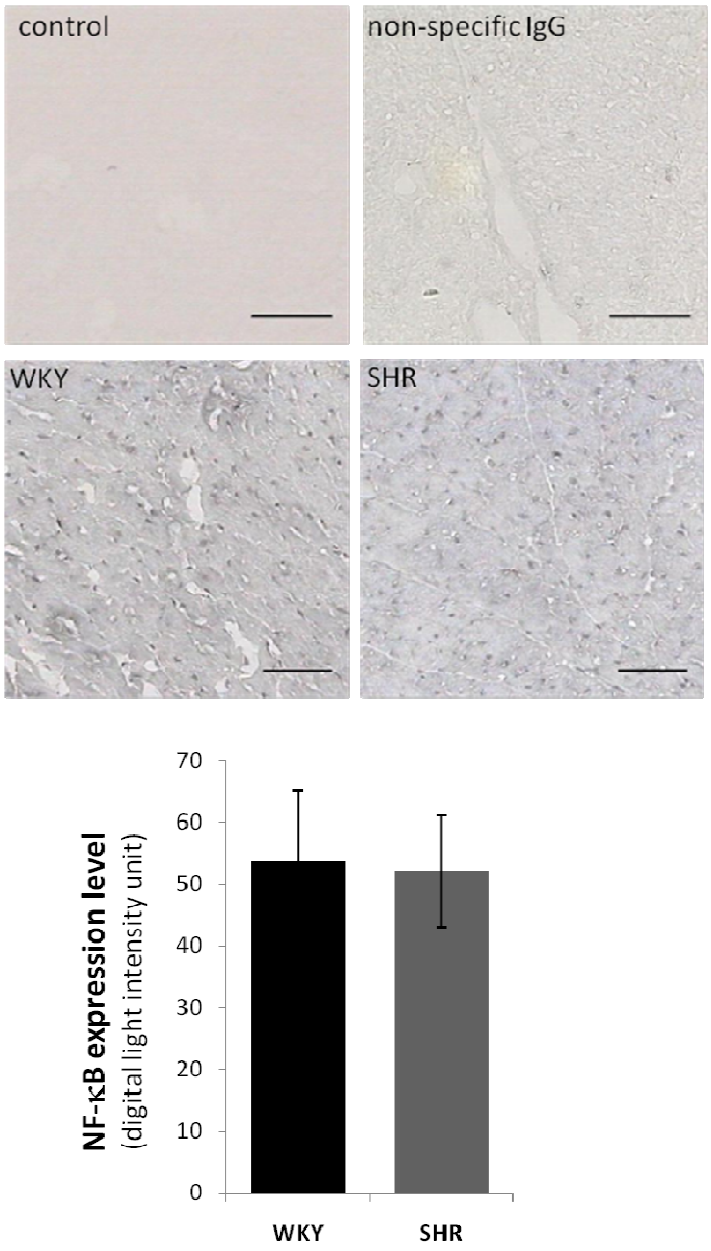

Figure 3-2. Immunohistochemical sections showing NF-κB expression level in myocardium. For explanation of cases, images, and measurements please see Figure 2 legend. Scale bar = 100 μm. N=4 rats for each group. There are no differences between WKY and SHR rats in NF-κB expression level in the myocardium.

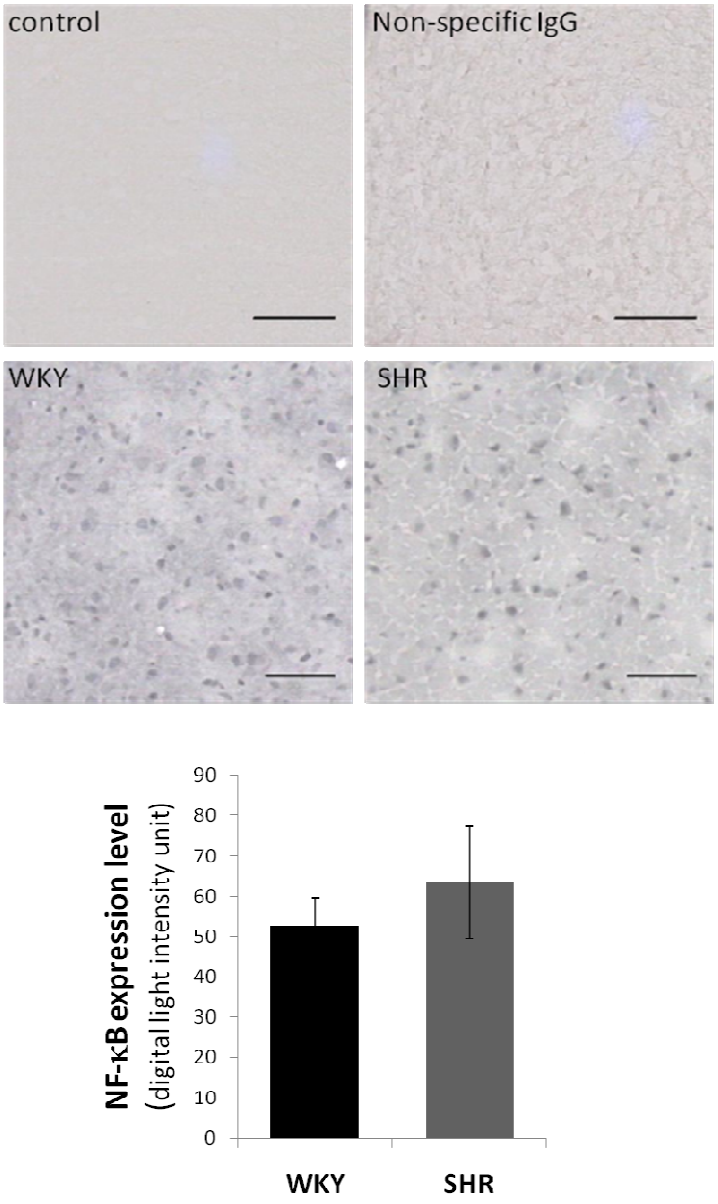

Figure 3-3. Immunohistochemical sections showing NF-κB expression level in cerebral cortex. For explanation of cases, images, and measurements please see Figure 2 legend. Scale bar = 100 μm. N=4 rats for each group. There are no significant differences of NF-κB expression level in cerebral cortex detected between WKY and SHR rats.

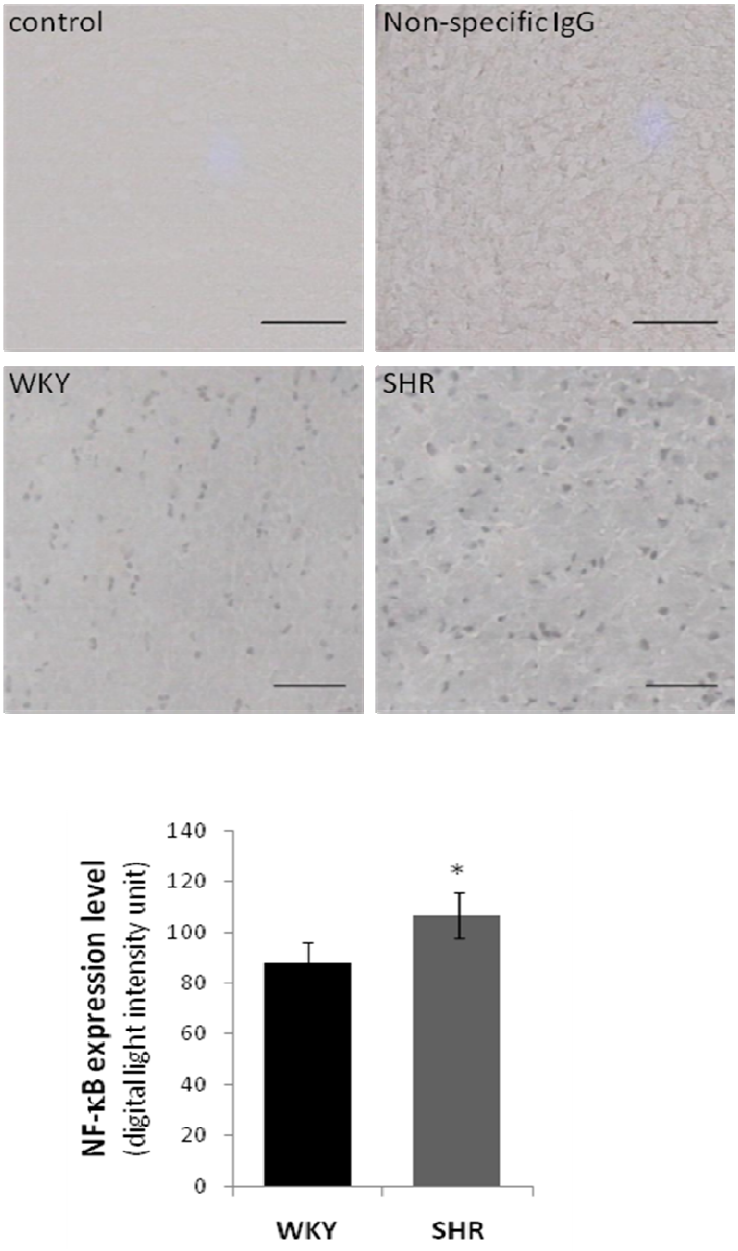

Figure 3-4. Immunohistochemical sections showing NF-κB expression level in hypothalamus region of the brain. For explanation of cases, images, and measurements please see Figure 2 legend. Scale bar = 100 μm. The SHR has higher expression of NF-κB p65 subunit in the hypothalamus. N=4 rats for each group. *p <0.05 compared to WKY in student's t-test.

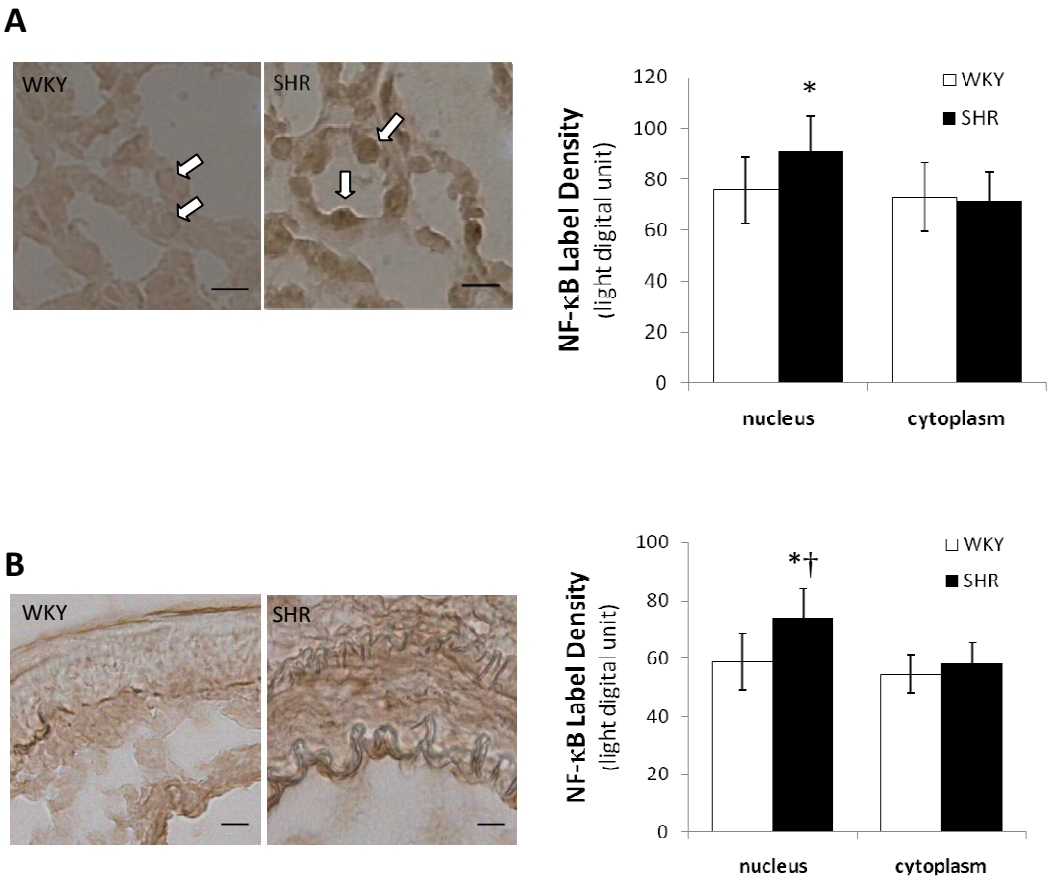

Figure 3-5. (Left panels) Micrographs of immunohistochemical sections. (Right bar graphs) NF-κB label expression levels in the nucleus (arrows) and the cell cytoplasm determined by optical density measurements in renal tubular cells **(A)** and in arterioles of the kidney **(B)**. SHR has a higher NF-κB label density in the nucleus both in renal tissue cells and blood vessel wall, and there are no differences in cytoplasm between WKY and SHR, indicating NF-κB nuclear translocation in the SHR. *p <0.05 compared to WKY nucleus, †p<0.05 compared to SHR cytoplasm in student's t-test with antibody against NF-κB in WKY and SHR kidney. N=5 rats for each group. Scale bar = 25 μm.

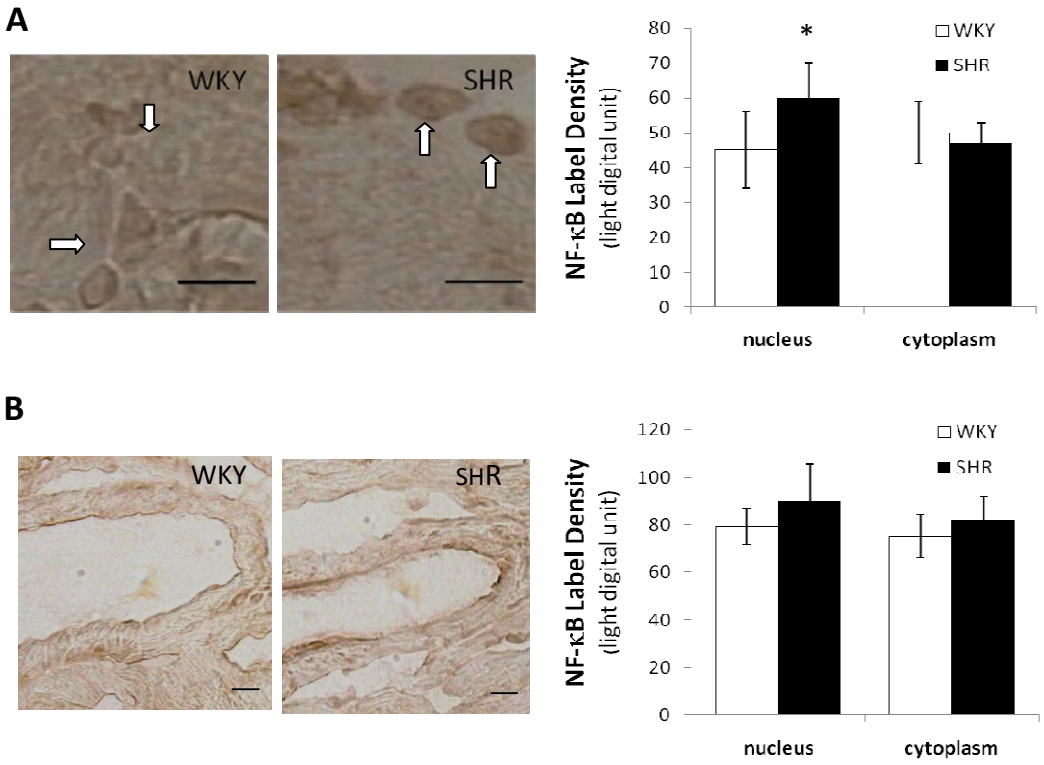

Figure 3-6. (Left panels) Micrographs of immunohistochemical sections. (Right bar graphs) NF-κB label expression levels in the nucleus (arrows) and the cell cytoplasm determined by optical density measurements in cardiac muscle cells **(A)** and in arterioles of the heart **(B)**. Compared to the WKY, the SHR has a higher NF-κB label density in the nucleus of myocardial cells, and there are no differences in cytoplasm between the strains, indicating NF-κB translocation in the SHR. There are no significant differences of the NF-κB label density between WKY and SHR in blood vessels of the myocardium. *p <0.05 compared to SHR cytoplasm in student's t-test with antibody against NF-κB in WKY and SHR myocardium. N=5 rats for each group. Scale bar = 25 μm.

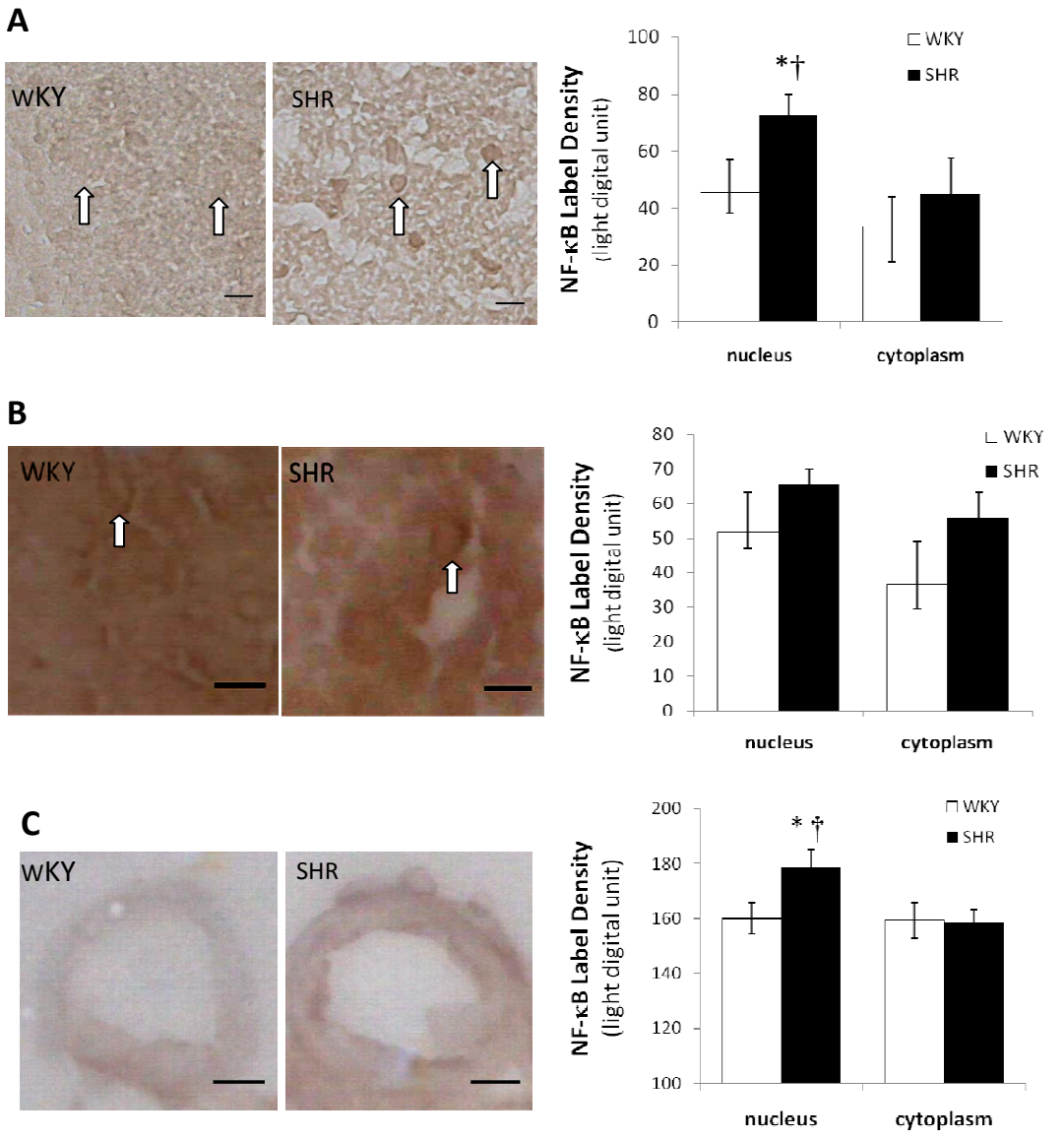

Figure 3-7. (Left panels) Micrographs of immunohistochemical sections. (Right bar graphs) NF-κB label expression levels in the nucleus (arrows) and the cell cytoplasm determined by optical density measurements in tissue parenchyma of hypothalamus **(A)** and in cerebral cortex **(B)** and in arterioles of brain. **(C)** Compared to the WKY, the SHR has a higher NF-κB label density in the nucleus of blood vessel wall, and there are no differences in cytoplasm between the strains, indicating NF-κB translocation in the SHR. There are no significant differences of the NF-κB label density between WKY and SHR in the brain parenchyma. *$p<0.05$ compared to WKY nucleus, †$p < 0.01$ compared to SHR cytoplasm in student's t-test with antibody against NF-κB in WKY and SHR brain. N=5 rats for each group. Scale bar = 25 μm.

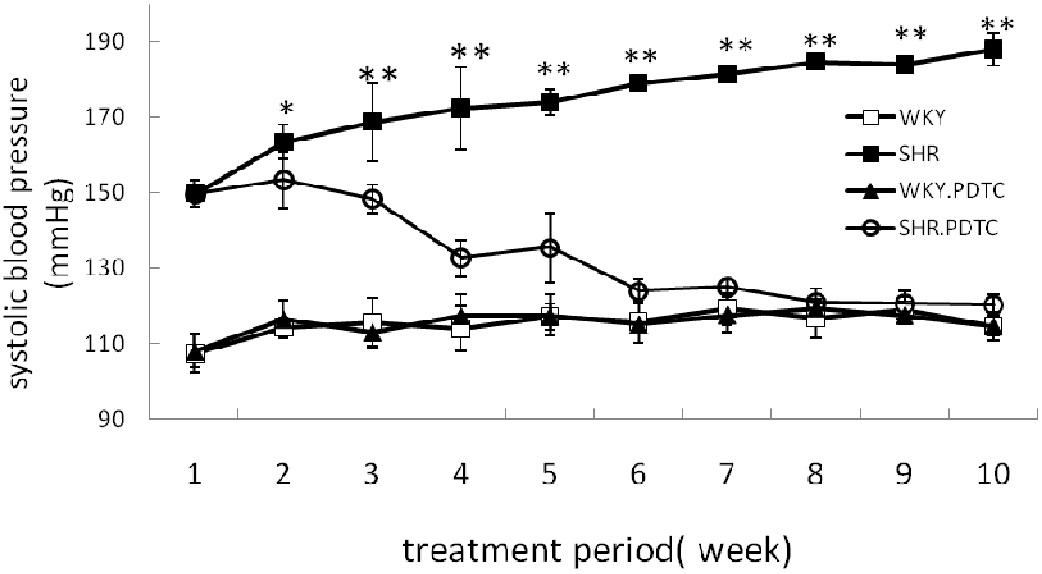

Figure 3-8 Systolic blood pressure in conscious age-matched SHR and WKY with and without treatment with pyrrolidine dithiocarbamate (PDTC). *$p<0.05$ compared to treated SHR in student's t-test. **$p<0.01$ compared to treated SHR in student's t-test. The time courses of blood pressure in treated-SHR during the treatment also showed a significant difference compared to the non-treated SHR by two-factor ANOVA ($p<0.01$).

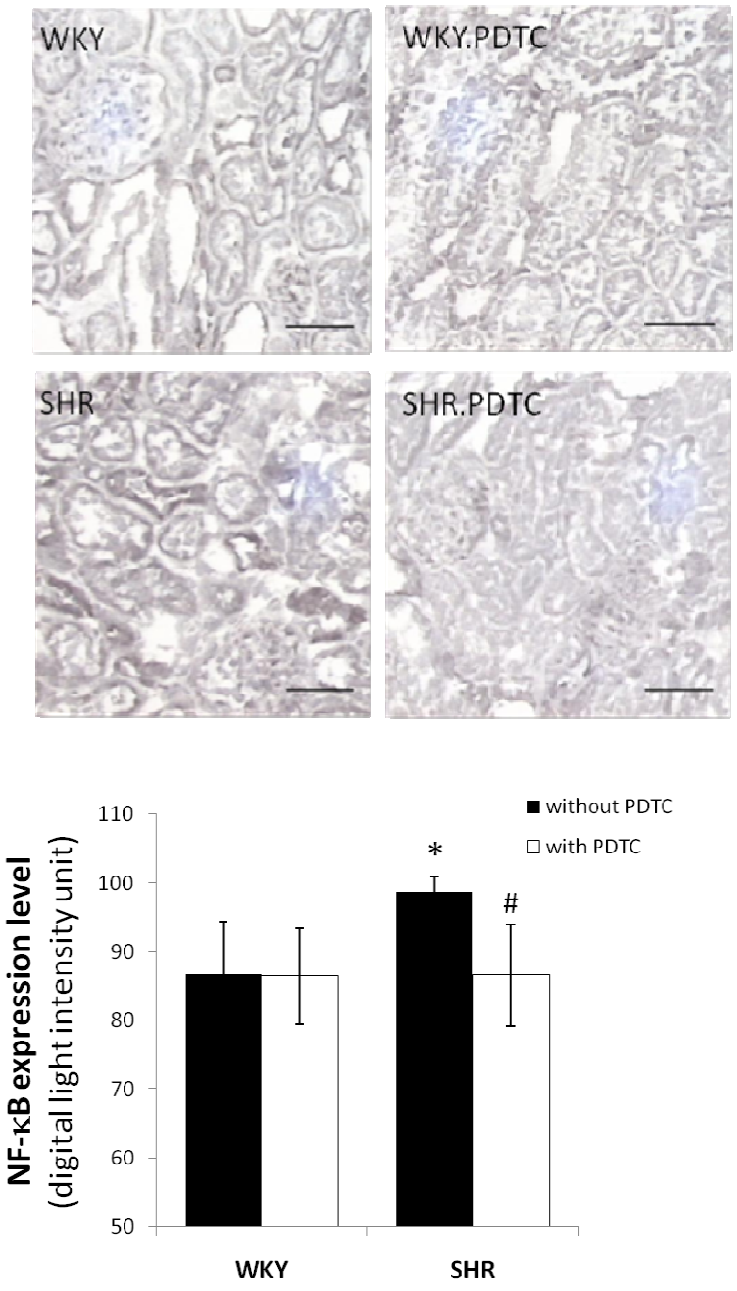

Figure 3-9. Micrographs (top panels) and optical density measurements (bar graph below) of NF-κB expression level in renal glomerular and tubulointerstitial areas without (left top images) and with (right) PDTC treatment. For explanation of cases, images, and measurements please see Figure 2 legend. The PDTC-treated SHR has lower NF-κB expression level compared to non-treated SHR. *p <0.05 compared to WKY. #p <0.05 compared to non-treated SHR in student's t-test. N=4 rats for non-treated group. N=5 rats for treated group. Scale bar = 100 μm.

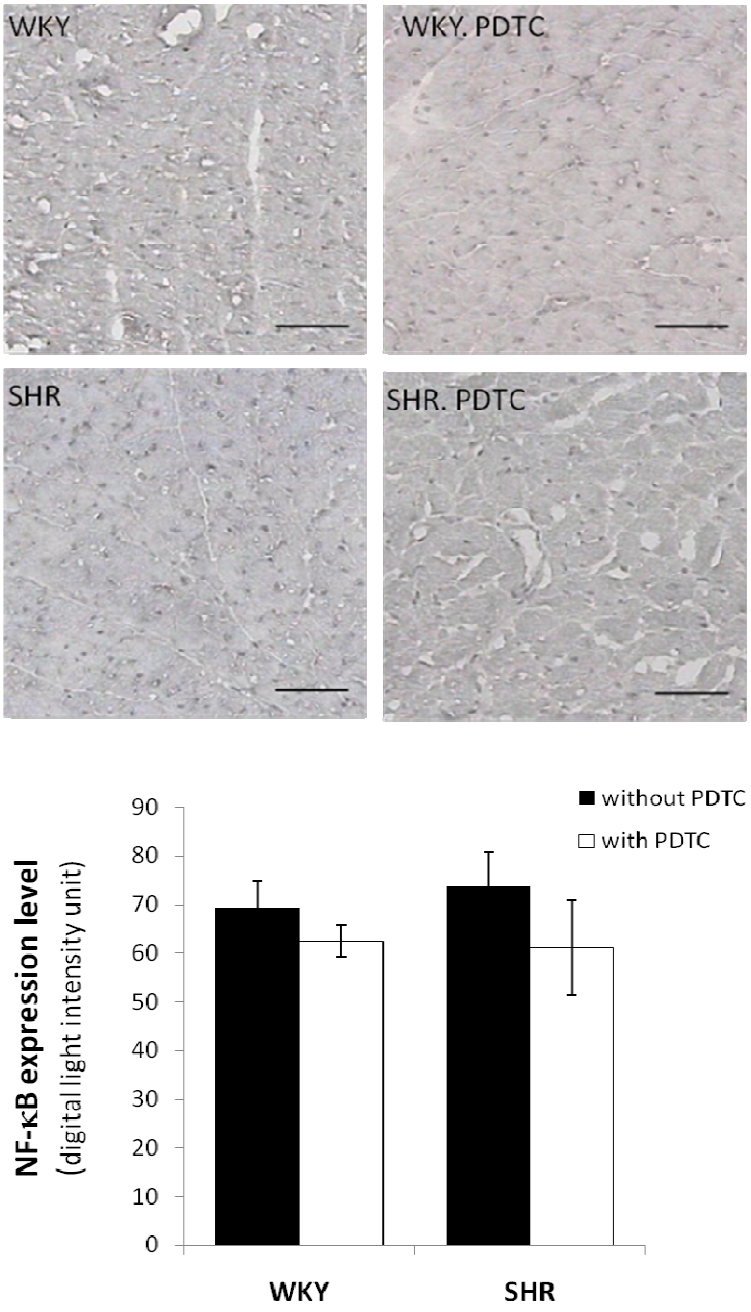

Figure 3-10. Micrographs (top panels) and optical density measurements (bar graph below) of NF-κB expression levels in myocardium without (left top images) and with (right) PDTC treatment. For explanation of cases, images, and measurements please see Figure 2 legend. There are no significant differences detected between both WKY and SHR and after treatment. N=4 rats for non-treated group. N=5 rats for treated group. Scale bar = 100 μm.

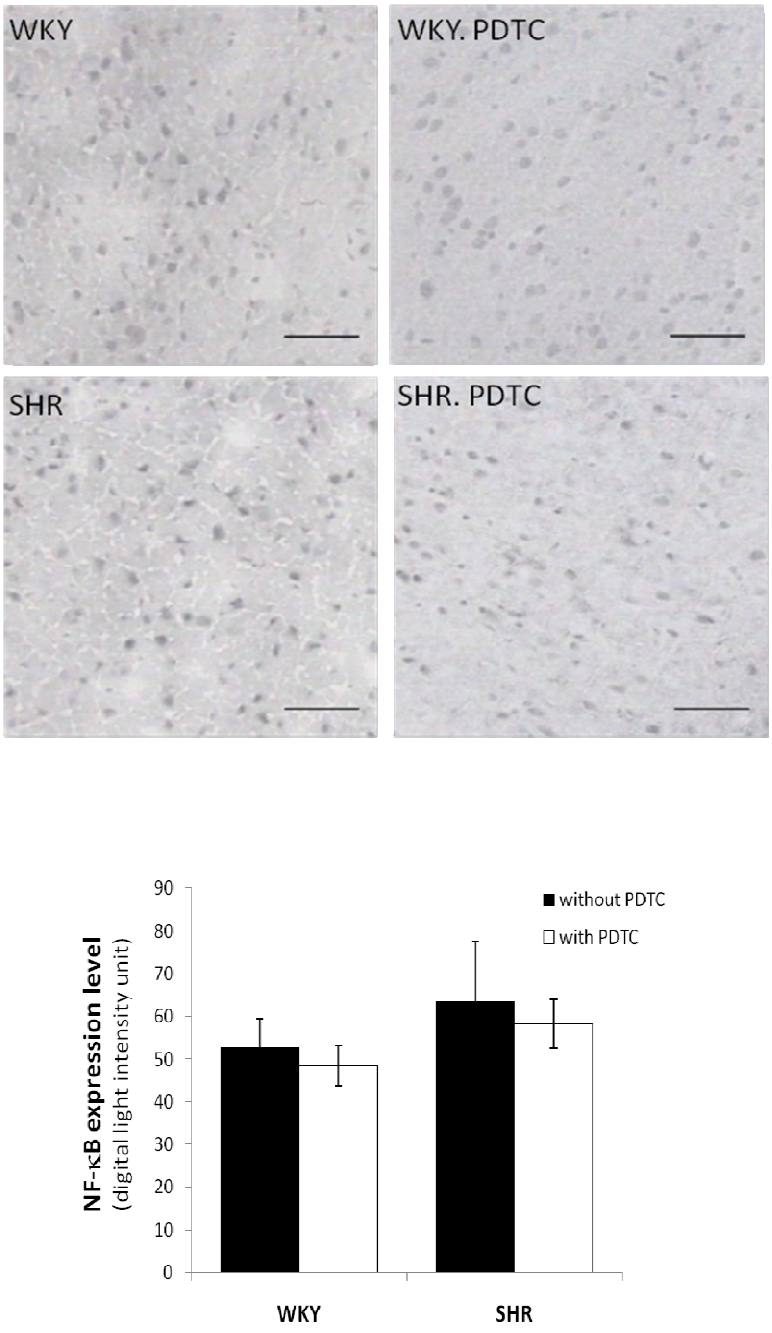

Figure 3-11. Micrographs (top panels) and optical density measurements (bar graph below) of NF-κB expression levels in cerebral cortex without (left top images) and with (right) PDTC treatment. For explanation of cases, images, and measurements please see Figure 2 legend. There are no significant differences detected between both WKY and SHR and after treatment. N=4 rats for non-treated group. N=5 rats for treated group. Scale bar = 100 μm.

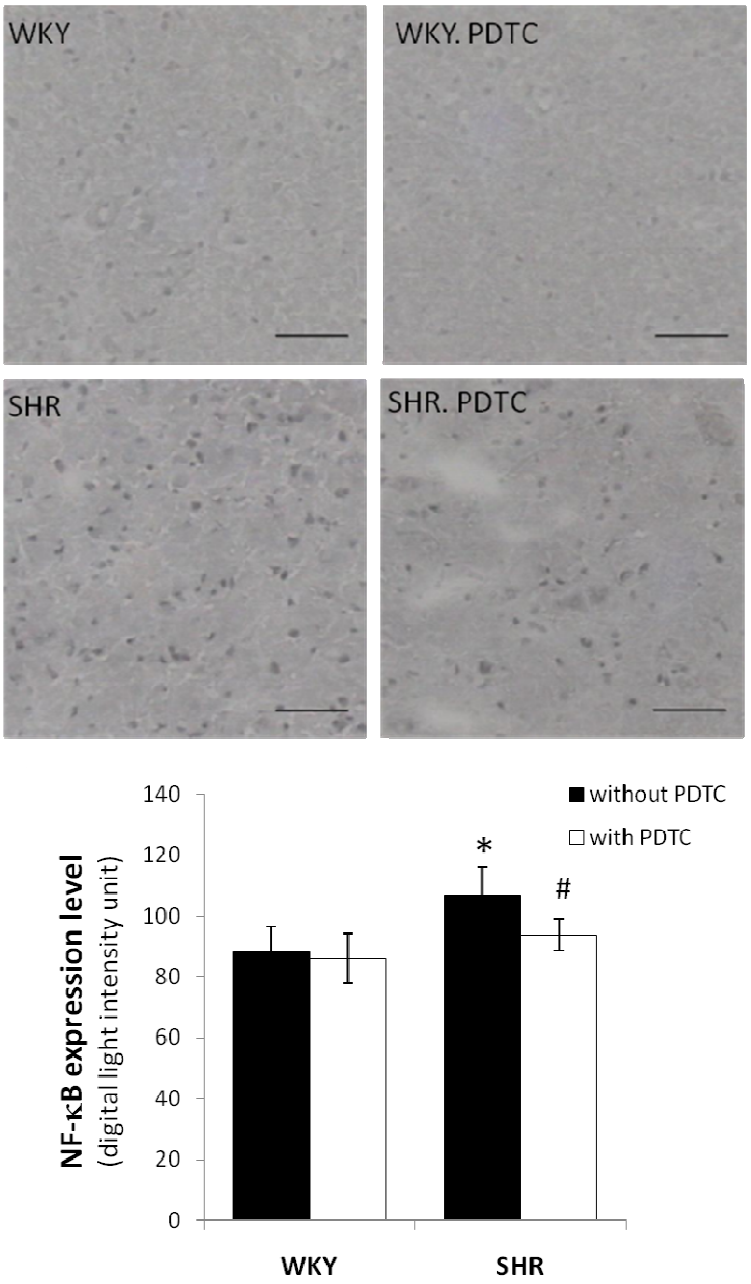

Figure 3-12. Micrographs (top panels) and optical density measurements (bar graph below) of NF-κB expression levels in hypothalamus region of brain without (left top images) and with (right) PDTC treatment. For explanation of cases, images, and measurements please see Figure 2 legend. The PDTC-treated SHR has lower NF-κB expression level compared to non-treated SHR. *p <0.05 compared to WKY, #p <0.05 compared to non-treated SHR in student's t-test. N=4 rats for non-treated group. N=5 rats for treated group. Scale bar = 100 μm.

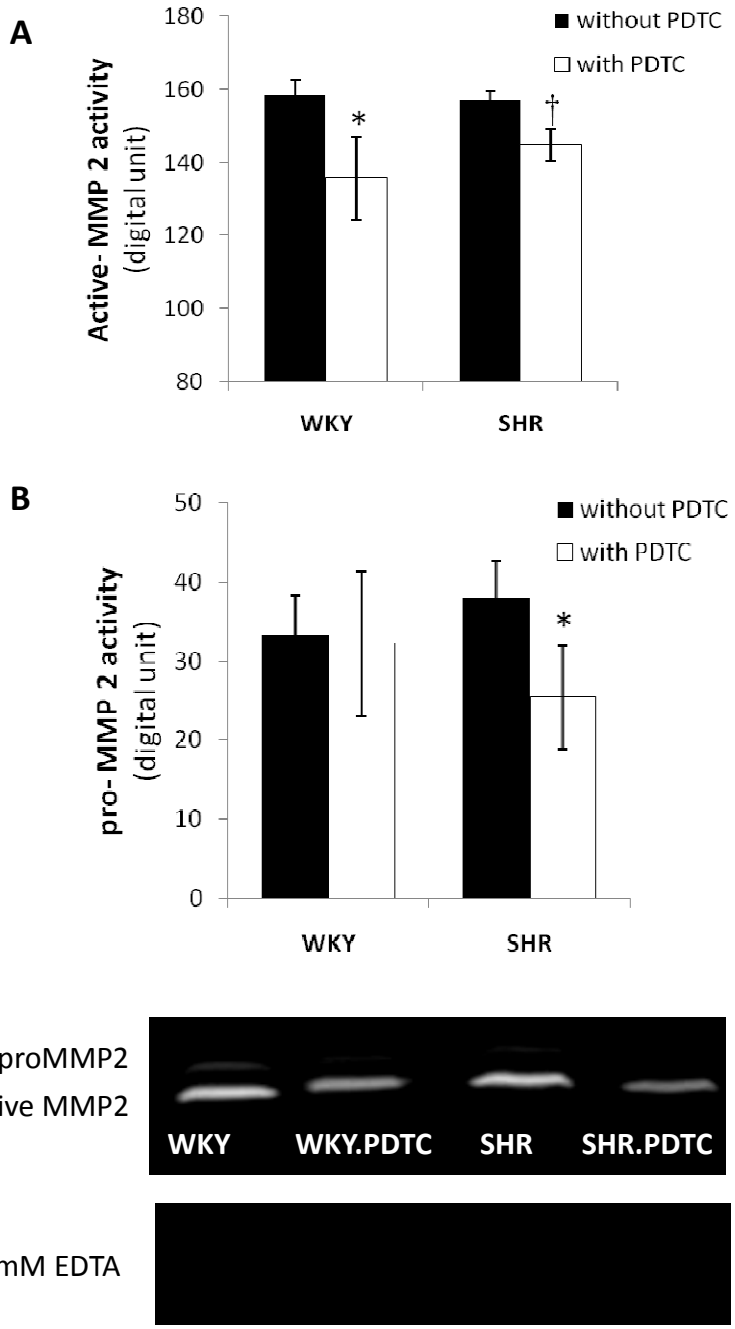

Figure 3-13. MMP 2 activity values in WKY and SHR plasma without and with PDTC treatment measured by gelatine zymography. The protease activity in plasma was confirmed with gel zymography using molecular weight standards. (A) Active form of MMP-2 (lower band, 66kDa). *p <0.05 compared to non-treated WKY †p<0.05 compared to non-treated SHR in student's t-test. (B) Pro-MMP-2(upper band, 72kDa). *p <0.05 compared to non-treated SHR in student's t-test. As control, all MMP activity is blocked in-vitro by metal chelation (EDTA) (bttom). N=4 rat plasmas in each animal group

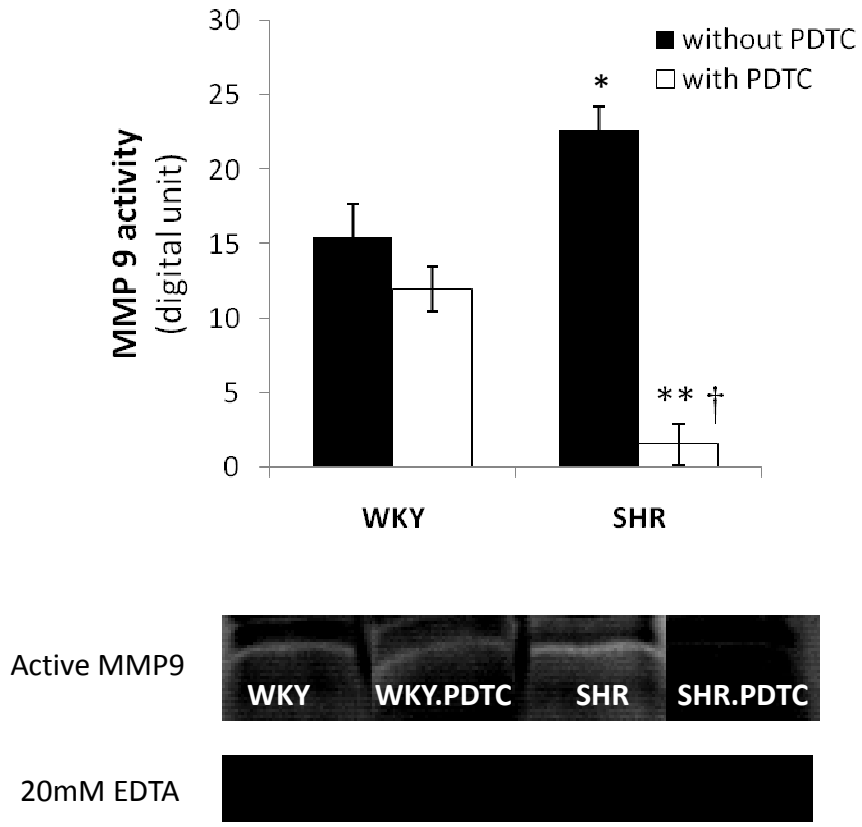

Figure 3-14. MMP 9 (86kDa) activity in WKY and SHR plasma without and with PDTC treatment determined by gelatine zymography. The protease activity in plasma was confirmed with gel zymography using molecular weight standards for confirmation. As control, all MMP activity is blocked in-vitro by metal chelation (EDTA). *p <0.05 compared to non-treated WKY, †p <0.05 compared to treated WKY **p<0.01 compared to non-treated SHR in student's t-test. N=4 rats in each group.

Chapter 4 Discussion

The current results indicate that the nuclear transcription factor NF-κB is overexpressed in the SHR. Blockade of the NF-κB by PDTC treatment can suppress NF-κB expression level and attenuate systolic blood pressure in the SHR. The MMP-2 and MMP-9 activity in the SHR plasma have also been significantly decreased after the ten weeks treatment.

4.1 NF-κB Expression Level and Nuclear Translocation

To examine NF-κB expression level in this study we used immunohistochemistry with anti-NF-κB p65 antibody in combination with light absorption measurements as a way to quantify the protein levels. This approach permits detection of the transcription factor in different tissue regions (e.g. endothelial cells, versus mastcells or parenchymal cells), which in an alternative approach (e.g. Western analysis) is not possible at the microvascular level due to the need to homogenize the tissue. Separate measurements of the immunolabel density in the nucleus and in the cytoplasm can also be used to quantify nuclear translocation.

In kidney section, we found the SHR has elevated NF-κB expression in glomerular and tubulointerstitial areas. Also, the NF-κB expression is significantly higher ($p < 0.05$) in SHR nucleus than in cytoplasm while there is no difference in WKY. When activation of NF-κB occurred, free NF-κB is released from IκB and translocated into the nucleus. Thus, higher expression levels in the nucleus indicates

NF-κB translocation and possible nuclear binding. The results we found are consistent with the results from previous results in a renal model of hypertension (38). This showed that activation of NF-κB may be a general mechanism involving in hypertension.

Since myocardial infarction and left ventricular hypertrophy are strongly associated with hypertension (8,32), we also examine NF-κB expression level in myocardium. Although we did not see significantly increased expression in SHR than WKY, there is higher expression level found in SHR nucleus. This result shows that even total NF-κB protein level is not increased, NF-κB activation is still significant in myocardium in hypertension. The SHR like other models of hypertension exhibit extensive apoptosis (26,30). Therefore our results have to be looked at in the context of cell apoptosis. Cells that undergo apoptosis loose the ability to synthesize new proteins and therefore the group of cells that are being analyzed in our experiments are merely those cells still capable of protein synthesis.

To study NF-κB expression in the brain, we look at two different regions, which are the cerebral cortex and the hypothalamus. The cerebral cortex, a layer of the brain often referred to as gray matter, plays a key role in memory and perceptual function, such as thinking, understanding, and language. The hypothalamus is involved in diencephalon, which lies between the brain stem and the cerebrum. It is the center for homeostasis and responsible for various endocrine function. In this study, we found NF-κB is significantly activated only in the SHR hypothalamus region but not in the cerebral cortex. This evidence may suggest that hypertensive

pathology is more related to dysfunction hypothalamus since the output from the hypothalamus can influence nervous system and endocrine system, which is associated with blood pressure control (48).

Besides the nuclear translocation in tissue area, we also studied NF-κB activation in blood vessels in different tissues. The results show that there are significant NF-κB nucleus translocations in kidney and brain vessels. There is a possibility that NF-κB activation in vessels in these tissues may result in endothelial dysfunction and further organ damage, such as renal failure and stroke.

4.2 Effect of PDTC Treatment

4.2.1 Systolic Blood Pressure Measurement

Several studies have applied PDTC in different hypertension models and shown improvement, including attenuation of blood pressure, improving cardiac hypertrophy, reducing cardiac mass and reducing inflammatory cells infiltration in heart and kidney (20,35,40). In this study, we followed the treatment protocol as in previous studies but increased the dose to 150 mg per kg per day. After two weeks, the systolic blood pressure was already significantly decreased in PDTC-treated SHR compared to non-treated SHR. After a 10 week treatment period, the systolic blood pressure was decreased on average by 36% in PDTC-treated SHR and hadvalue similar to normotensive WKY rats.

In order to confirm the tail-cuff measurements of systolic blood pressure with PDTC treatment, we randomly chose one PDTC-treated SHR and un-treated SHR and cannulated the femoral artery under local anesthesia to directly measure

systolic blood pressure after 5 weeks treatment. The systolic blood pressure of non-treated SHR was 160 mmHg, compared to 106 mmHg in the PDTC-treatedSHR. These values are similar to those we got from tail-cuff measurement.

Gupta et al. (2005) applied PDTC at a dose of 25 mg/kg/day for 10 weeks. The treated-SHR decreased their systolic blood pressure by 9.6% (20). Rodriguez-Iturbe et al. (2005)(40) treated animals with 100 mg/kg/day for 18 weeks. At the end of the treatment, the systolic blood pressure of the PDTC-treated SHR was decreased by 36%,a level that is similar to our measurements. Since we can reach the same suppression of blood pressure with shorter treatment period compared to the study by Rodriguez-Iturbe et al. (2005), it indicates that PDTC inhibition is a dose-dependent event (45). A higher dose may have faster effect on blood pressure.

4.2.2 NF-κB Expression Levels

Gupta el al (2005)(20) found inhibition of NF-κB can attenuate hypertrophy, however, we didn't see significantly decreased NF-κB expression in the myocardium after PDTC treatment. It can be explained that PDTC may possibly affect other factor that can suppress blood pressure without changing the total NF-κB protein level. In the kidney and the hypothalamus region of the brain, only the SHR is affected by PDTC treatment with a decreased level of NF-κB expression. The WKY ratsmaintained similar NF-κB expression level with and without treatment, suggesting that the SHR is more sensitive to the treatment. The results are

also consistent with my previous data without treatment, in which NF-κB expression levels were different between WKY and SHR in only kidney and hypothalamus but not myocardium or cerebral cortex.

4.2.3 MMP-2 and MMP-9 Activities

The gelatin gel zymography indicate different MMP activities, but only the active form of MMP-2, the pro-form of MMP-2 and the active form of MMP-9 were sufficiently clear for quantification in this study.

The result shows that the MMP-2 activities were suppressed by PDTC treatment in both WKY and SHR. But the pro-form MMP-2 was attenuated only in the SHR. Comparing WKY and SHRs, no significant difference was present in the MMP-2 activity. Some studies have shown increased MMP-2 in SHR than in WKY; however, most studies were focused on either mRNA level or protein level (7,24), different from the enzyme activity.

The SHR exhibited an elevated MMP-9 activity compared to WKY. After PDTC treatment the MMP-9 activity was attenuated only in SHR but not WKY, similar to the MMP-2 results. After PDTC treatment, SHR value is lower than before treatment but not WKY. Again, this result indicates that the SHR is more responsive to PDTC treatment, possibly due to its different pathway of NF-κB triggering MMP expression. Genetic analysis have already found NF-κB binding site in promoter region in MMP-9 (5), which can explain the suppression effect of PDTC on MMP-9 activity.

Chapter 5 Conclusion

In this study, we found NF-κB expression or activation are enhanced in kidney, heart, and brain. This suggests that NF-κB is associated with inflammation and important organ dysfunction in hypertension. The findings in this study are also consistent with our hypotheses that PDTC can suppress systolic blood pressure in hypertensive rats and downregulate the NF-κB expression level. The attenuation of MMP-2 and -9 activities by PDTC also shows the possible role of NF-κB in triggering increased MMP activity in hypertension. Further investigation of pathogenesis process such as receptor cleavage may be required to show the stronger association between NF-κB and end-organ damage in hypertensive model.

References

1. Allan A.J., Docherty A.J., Barker P.J., Huskisson N.S., Reynolds J.J. and Murphy G. Binding of gelatinases A and B to type-I collagen and other matrix components. Biochem J 209(pt1):299-306, 1995.

2. Baldwin A.S. The NF-kB and IkB Proteins: New Discoveries and Insights. annurev.immunol 14(1):649-681, 1996.

3. Bataillard A., Renaudin C. and Sassard J. Silica attenuates hypertension in Lyon hypertensive rats. J Hypertens 13(12):1581-1584, 1995.

4. Bautista L.E. Inflammation, endothelial dysfunction, and the risk of high blood pressure: epidemiologic and biological evidence. J Hum Hypertens 17(4):223-230, 2003.

5. Bond M., Chase A.J., Baker A.H. and Newby A.C. Inhibition of transcription factor NF-{kappa}B reduces matrix metalloproteinase-1, -3 and -9 production by vascular smooth muscle cells. Cardiovasc Res. 50(3):556-565, 2001.

6. Boos C.J. and Lip G.Y.H. Is hyertenstion an inflammatory process? Curr Pharm Des. 12(13):1623-1635, 2006.

7. Camp T.M., Smiley L.M., Hayden M.R. and Tyagi S.C. Mechanism of matrix accumulation and glomerulosclerosis in spontaneously hypertensive rats. J Hypertens 21(9):1719-1727, 2003.

8. Chanutin A. and Barksdale E.E. Experimental renal insufficiency produced by partial nephrectomy: II. relelationship of left ventricular hypertrophy, the width of the cardiac muscle fiber and hypertension in the rat. Arch Intern Med. 52(5):739-751, 1933.

9. Chen C.C., Rosenbloom C.L., Anderson D.C. and Manning A.M. Selective inhibition of E-selectin, vascular cell adhesion molecule-1, and intercellular adhesion molecule-1 expression by inhibitors of I kappa B-alpha phosphorylation. J Immunol. 155(7):3538-3545, 1995.

10. Chen F., Castranova V., Shi X. and Demers L.M. New Insights into the Role of Nuclear Factor-{kappa}B, a Ubiquitous Transcription Factor in the Initiation of Diseases. Clin Chem. 45(1):7-17, 1999.

11. Clark I.M., Swingler T.E., Sampieri C.L. and Edwards D.R. The regulation of matrix metalloproteinases and their inhibitors. Int J Biochem Cell Biol. 40(6-7):1362-1378, 2008.

12. Cushman W. JNC-7 guidelines: are they still relevant? Curr Hypertens Rep. 9(5):380-386, 2007.

13. Dahl L.K., Heine M. and Tassinari L. Effects of chronic excess salt ingestion. Evidence that genetic factors play an important role in susceptibility to experimental hypertension. J. Exp. Med. 115(6):1173-1190, 1962.

14. DeLano F.A., Forrest M.J. and Schmid-Schönbein G.W. Attenuation of oxygen free radical formation and tissue injury during experimental inflammation by P-selectin blockade. Microcirculation 4(3):349-357, 1997.

15. DeLano F.A. and Schmid-Schönbein G.W. Proteinase Activity and Receptor Cleavage: Mechanism for Insulin Resistance in the Spontaneously Hypertensive Rat. Hypertension 52(2):415-423, 2008.

16. Fabunmi R.P., Baker A.H., Murray E.J., Booth R.F. and Newby A.C. Divergent regulation by growth factors and cytokines of 95 kDa and 72 kDa gelatinases and tissue inhibitors or metalloproteinases-1, -2, and -3 in rabbit aortic smooth muscle cells. Biochem J 315(Pt1):335-342, 1996.

17. Galis Z.S. and Khatri J.J. Matrix Metalloproteinases in Vascular Remodeling and Atherogenesis: The Good, the Bad, and the Ugly. Circ Res. 90(3):251-262, 2002.

18. Gilmore T.D. Introduction to NF-kappaB: players, pathways, perspectives. Oncogene 25(51):6680-6684, 2006.

19. Gilmore T.D. and Herscovitch M. Inhibitors of NF-kappaB signaling: 785 and counting. Oncogene 25(51):6887-6899, 2006.

20. Gupta S., Young D. and Sen S. Inhibition of NF-kappaB induces regression of cardiac hypertrophy, independent of blood pressure control, in spontaneously hypertensive rats. Am J Physiol Heart Circ Physiol. 289(1):H20-29, 2005.

21. Henke N., Schmidt-Ullrich R., Dechend R., Park J.K., Qadri F., Wellner M., Obst M., Gross V., Dietz R., Luft F.C., Scheidereit C. and Muller D.N. Vascular endothelial cell-specific NF-kappaB suppression attenuates

hypertension-induced renal damage. Circ Res. 101(3):268-276, 2007.

22. Hong H.J., Loh S.H. and Yen M.H. Suppression of the development of hypertension by the inhibitor of inducible nitric oxide synthase. Br J Pharmacol. 131(3):631-637, 2000.

23. Hong H.J., Wu C.C. and Yen M.H. Pyrrolidine dithiocarbamate improves the septic shock syndromes in spontaneously hypertensive rats. Clin Exp Pharmacol Physiol. 25(7-8):600-606, 1998.

24. Hultstrom M., Leh S., Skogstrand T. and Iversen B.M. Upregulation of Tissue Inhibitor of Metalloproteases-1 (TIMP-1) and Procollagen-N-Peptidase in Hypertension-Induced Renal Damage. Nephrol Dial Transplant 2007(0):1-8, 2007.

25. Kim C.H., Kim J.H., Hsu C.Y. and Ahn Y.S. Zinc is required in pyrrolidine dithiocarbamate inhibition of NF-kappaB activation. FEBS letters 449(1):28-32, 1999.

26. Kobayashi N., DeLano F.A. and Schmid-Schönbein G.W. Oxidative Stress Promotes Endothelial Cell Apoptosis and Loss of Microvessels in the Spontaneously Hypertensive Rats. Arterioscler Thromb Vasc Biol. 25(10):2114-2121, 2005.

27. Kusano K., Miyaura C., Inada M., Tamura T., Ito A., Nagase H., Kamoi K. and Suda T. Regulation of Matrix Metalloproteinases (MMP-2, -3, -9, and -13) by Interleukin-1 and Interleukin-6 in Mouse Calvaria: Association of MMP Induction with Bone Resorption. Endocrinology 139(3):1338-1345, 1998.

28. Li J.J., Fang C.H. and Hui R.T. Is hypertension an inflammatory disease? Med Hypotheses. 64(2):236-240, 2005.

29. Li Q., Antwerp D.V., Mercurio F., Lee K.-F. and Verma I.M. Severe Liver Degeneration in Mice Lacking the IB Kinase 2 Gene. 1999, pp. 321-325.

30. Lim H.H., DeLano F.A. and Schmid-Schöbein G.W. Life and Death Cell Labeling in the Microcirculation of the Spontaneously Hypertensive Rat. J Vasc Res. 38(3):228-236, 2001.

31. Luft F.C., Mervaala E., Muller D.N., Gross V., Schmidt F., Park J.K.,

Schmitz C., Lippoldt A., Breu V., Dechend R., Dragun D., Schneider W., Ganten D. and Haller H. Hypertension-Induced End-Organ Damage : A New Transgenic Approach to an Old Problem. Hypertension 33(1):212-218, 1999.

32. Madhavan S., Ooi W.L., Cohen H. and Alderman M.H. Relation of pulse pressure and blood pressure reduction to the incidence of myocardial infarction. Hypertension 23(3):395-401, 1994.

33. Maulik N., Sato M., Price B.D. and Das D.K. An essential role of NF[kappa]B in tyrosine kinase signaling of p38 MAP kinase regulation of myocardial adaptation to ischemia. FEBS letters 429(3):365-369, 1998.

34. Mayo M.W., Wang C.-Y., Cogswell P.C., Rogers-Graham K.S., Lowe S.W., Der C.J. and Baldwin A.S., Jr. Requirement of NF-{kappa}B Activation to Suppress p53-Independent Apoptosis Induced by Oncogenic Ras. Science (New York, N.Y 278(5344):1812-1815, 1997.

35. Muller D.N., Dechend R., Mervaala E.M., Park J.K., Schmidt F., Fiebeler A., Theuer J., Breu V., Ganten D., Haller H. and Luft F.C. NF-kappaB inhibition ameliorates angiotensin II-induced inflammatory damage in rats. Hypertension 35(1 Pt 2):193-201, 2000.

36. Okamoto K. and Aoki K. Development of a strain of spontaneously hypertensive rats. Jap. Circul. 27:282-293, 1963.

37. Pinkus R., Weiner L.M. and Daniel V. Role of Oxidants and Antioxidants in the Induction of AP-1, NF-kappa B, and Glutathione S-Transferase Gene Expression. J Biol Chem 271(23):13422-13429, 1996.

38. Quiroz Y., Bravo J., Herrera-Acosta J., Johnson R.J. and Rodriguez-Iturbe B. Apoptosis and NF[kgr]B activation are simultaneously induced in renal tubulointerstitium in experimental hypertension. Kidney Int 64(S86):S27-S32, 2003.

39. Raffetto J.D. and Khalil R.A. Matrix metalloproteinases and their inhibitors in vascular remodeling and vascular disease. Biochem Pharmacol. 75(2):346-359, 2008.

40. Rodriguez-Iturbe B., Ferrebuz A., Vanegas V., Quiroz Y., Mezzano S. and Vaziri N.D. Early and Sustained Inhibition of Nuclear Factor-{kappa}B Prevents Hypertension in Spontaneously Hypertensive Rats. J Pharmacol Exp Ther. 315(1):51-57, 2005.

41. Rodriguez-Iturbe B., Quiroz Y., Nava M., Bonet L., Chavez M., Herrera-Acosta J., Johnson R.J. and Pons H.A. Reduction of renal immune cell infiltration results in blood pressure control in genetically hypertensive rats. Am J Physiol Renal Physiol 282(2):F191-201, 2002.

42. Satriano J. and Schlondorff D. Activation and attenuation of transcription factor NF-kB in mouse glomerular mesangial cells in response to tumor necrosis factor-alpha, immunoglobulin G, and adenosine 3':5'-cyclic monophosphate. Evidence for involvement of reactive oxygen species. J Clin. Invest. 94(4):1629-1636, 1994.

43. Schmid-Schönbein G.W. Analysis of inflammation. Annu Rev Biomed Eng. 8:93-131, 2006.

44. Schmid-Schönbein G.W., Seiffge D., DeLano F.A., Shen K. and Zweifach B.W. Leukocyte counts and activation in spontaneously hypertensive and normotensive rats. Hypertension 17(3):323-330, 1991.

45. Schreck R., Meier B., Mannel D.N., Droge W. and Baeuerle P.A. Dithiocarbamates as potent inhibitors of nuclear factor kappa B activation in intact cells. J Exp Med. 175(5):1181-1194, 1992.

46. Sen R. and Baltimore D. Multiple nuclear factors interact with the immunoglobulin enhancer sequences. Cell 46(5):705-716, 1986.

47. Shen K., DeLano F.A., Zweifach B.W. and Schmid-Schönbein G.W. Circulating Leukocyte Counts, Activation, and Degranulation in Dahl Hypertensive Rats. Circu Res. 76(2):276-283, 1995.

48. Silverthorn D.U., Ober W.C., Garrison C.W., Silverthorn A.C. and Johnson B.R. Human Physiology: an integrated approach. San Francisco, CA, Daryl Fox, 2004.

49. Spinale f.G. Matrix metalloproteinases: regulation and dysregulation in the failing heart. Circu Res. 90:520-530, 2002.

50. Sunderman Fw, Sr. Therapeutic properties of sodium diethyldithiocarbamate: its role as an inhibitor in the progression of AIDS. Ann Clin Lab Sci 21(1):70-81, 1991.

51. Verma I.M., Stevenson J.K., Schwarz E.M., Van Antwerp D. and Miyamoto S. Rel/NF-kappa B/I kappa B family: intimate tales of association and

dissociation. Genes Dev. 9(22):2723-2735, 1995.

52. Visse R. and Nagase H. Matrix Metalloproteinases and Tissue Inhibitors of Metalloproteinases: Structure, Function, and Biochemistry. Circu Res. 92(8):827-839, 2003.